Introgression from extinct species facilitates adaptation to its vacated niche

David Frei[1,2*], Pascal Reichlin[1], Ole Seehausen[1,2], Philine G.D. Feulner[1,2]

[1]Department of Fish Ecology and Evolution, Centre of Ecology, Evolution and Biogeochemistry, EAWAG Swiss Federal Institute of Aquatic Science and Technology, Kastanienbaum, Switzerland

[2]Division of Aquatic Ecology and Evolution, Institute of Ecology and Evolution, University of Bern, Bern, Switzerland

[*]Corresponding author (david.frei@eawag.ch)

Anthropogenic disturbances of ecosystems are causing a loss of biodiversity at an unprecedented rate. Species extinctions often leave ecological niches underutilized, and their colonization by other species may require new adaptation. In Lake Constance, an endemic profundal whitefish species went extinct during a period of anthropogenic eutrophication. In the process of extinction, the deep-water species hybridized with three surviving whitefish species of Lake Constance, resulting in introgression of genetic variation that is potentially adaptive in deep-water habitats. Here, we sampled a water depth gradient across a known spawning ground of one of these surviving species, *Coregonus macrophthalmus*, and caught spawning individuals in greater depths (down to 90m) than historically recorded. We sequenced a total of 96 whole genomes, 11-17 for each of six different spawning depth populations (4m, 12m, 20m, 40m, 60m, and 90m), to document genomic intraspecific differentiation along a water depth gradient. We identified 52 genomic regions that are potentially under divergent selection between the deepest (90m) and all shallower (4-60m) spawning habitats. At 12 (23.1%) of these 52 loci, the allele frequency pattern across historical and contemporary populations suggests that introgression from the extinct species potentially facilitates ongoing adaptation to deep water. Our results are consistent with the syngameon hypothesis, proposing that hybridization between members of an adaptive radiation can promote further niche expansion and diversification. Furthermore, our findings demonstrate that introgression from extinct into extant species can be a source of evolvability enabling rapid adaptation to environmental change and may contribute to the ecological recovery of ecosystem functions after extinctions.

Keywords: Adaptive radiation, environmental change, extinction by hybridization, introgression, deep-water adaptation.

Introduction

The recovery of ecosystems from anthropogenic disturbances is a central factor to predict future consequences of environmental change on biodiversity (Malhi et al., 2020). When species go extinct due to anthropogenic disturbance, previously occupied niche space may become vacant (Prada et al., 2016). Thus, in communities lacking ecological redundancy, extinction can provide surviving species with previously unavailable ecological opportunity (Prada et al., 2016; Wellborn & Langerhans, 2015). Whether and within which time scale such vacant niche space that had previously been occupied by newly extinct species can be filled up again through niche expansion of related or newly emerging species is one critical aspect of determining the functional recovery of an ecosystem on an evolutionary timescale.

Degradation of ecosystems can result in species loss by either demographic decline, or by speciation reversal through the merging of several related species into a single hybrid population (Rhymer & Simberloff, 1996; Taylor, 2006; Tedesco et al., 2016). When reproductive isolation between species is mediated by features of the environment that interact with intrinsic lineage traits, environmental change can induce the loss of reproductive isolation, resulting in speciation reversal through introgressive hybridization (Seehausen, 2006; Seehausen, Takimoto, Roy, & Jokela, 2008; Taylor et al., 2006, Tedesco et al., 2016). Even when ecosystems are restored and thus disturbance was merely transient, speciation reversal can result in the loss of species. However, parts of the genetic variation that had once defined the lost species will then often have been transferred to surviving species through hybridization and introgression (Barlow et al., 2018; Kuhlwilm, Han, Sousa, Excoffier, & Marques-Bonet, 2019; Reilly, Tjahjadi, Miller, Akey, & Tucci, 2022). Thereby, speciation reversal can result in the functional extinction of taxa within a few generations (Rhymer & Simberloff, 1996; Taylor, 2006; Todesco et al., 2016; Vonlanthen et al., 2012), while some of

57 their genetic variation may persist within extant species (Frei et al., 2022; Gilman & Behm,
58 2011).

59 Rapid adaptation and speciation are often associated with re-assembling of old genetic
60 variation originating from hybridization (Marques, Meier, & Seehausen, 2019; Hamid,
61 Korunes, Beleza, & Goldberg, 2021; Moran et al., 2021). Examples include Darwin's finches
62 (Lamichhaney et al., 2015; Lamichhaney et al., 2016), cichlid fish (Irisarri et al., 2018; Meier
63 et al., 2017), *Lycaeides* butterflies (Nice et al., 2013) or *Helianthus* sunflowers (Rieseberg et
64 al., 2003). Hybridization is thought to promote ecological diversification and speciation
65 because it can generate new trait combinations suitable for utilizing resources that could not
66 be utilized before (Marques et al., 2019; Seehausen, 2004). Through these effects,
67 hybridization can fuel entire adaptive radiations, both the onset (Meier et al., 2017) and the
68 continuation of adaptive radiation beyond the first speciation events (Seehausen, 2004). In the
69 context of extinction by speciation reversal, introgressive hybridization during speciation
70 reversal might facilitate the adaptation of a surviving species to an extinct species' vacated
71 niche. Admixture variation generated through hybridization during speciation reversal might
72 be re-assembled into allelic combinations that are adaptive in the now unoccupied habitat
73 previously used by the extinct species. When some of the alleles derived from the extinct
74 species that evolved in response to selective pressures in its former habitat introgress into
75 surviving species, they might facilitate adaptation to the now vacant habitat within surviving
76 species. Such a scenario is in line with the syngameon hypothesis of adaptive radiations,
77 which predicts that hybridization between members of an existing adaptive radiation might
78 induce further adaptation and diversification (Seehausen, 2004).

79 The Alpine whitefish radiation provides an outstanding opportunity to study the
80 consequences of speciation reversal induced by severe but transient environmental change.
81 Reproductive isolation between sympatric Alpine whitefish species is maintained

predominantly by extrinsic (and possibly intrinsic) prezygotic and extrinsic postzygotic mechanisms (Vonlanthen et al., 2009; Woods et al., 2009; Ingram et al., 2012; Hudson et al., 2016). Many sympatric species differ in the water depth of spawning sites and show differential timing of spawning (Steinmann 1950). Some sympatric species overlap in both, yet retaining significant reproductive isolation, possibly due to behavioural mating preferences (Steinmann 1950; Hudson et al., 2016). Alpine whitefish species are highly sensitive to the alteration of the physiochemical habitat characteristics, because spawning niche differentiation and in turn reproductive isolation, is strongly dependent on the persistence of fine-scale depth-related differences in the specific lacustrine habitat (Vonlanthen et al., 2012; Hudson et al., 2016). Anthropogenic eutrophication during the last century weakened reproductive isolation between Alpine whitefish species, resulting in speciation reversal through introgressive hybridization (Frei et al., 2022; Vonlanthen et al., 2012).

In Lake Constance, a lake between the borders of Germany, Austria and Switzerland, four endemic whitefish species have been taxonomically described. The deep-water species *C. gutturosus* went extinct during eutrophication-induced speciation reversal (Vonlanthen et al., 2012). During the period of anthropogenic eutrophication, its deep-water spawning grounds were lost as a result of decreased oxygen concentrations (Nümann, 1972; Wahl & Löffler, 2009). The anoxic conditions at the water-sediment interface in deep benthic areas of the lake probably prevented successful reproduction of *C. gutturosus* and thereby contributed to its extinction (Deufel, Löffler, & Wagner 1986; Wahl & Löffler, 2009). Recent work demonstrated extensive introgression of this extinct species into all surviving members of the radiation (Frei et al., 2022). Introgression included potentially adaptive alleles that, before eutrophication, had been under positive selection in the extinct species (Frei et al., 2022). Today, oligotrophic conditions of the lake have been largely restored and deep-water habitats

are again accessible for fish. Yet, profundal habitats of Lake Constance are reported to be devoid of any whitefish (Alexander & Seehausen, 2021). However, the genetic variation that had evolved in the extinct deep-water species and introgressed into the extant species during eutrophication-induced speciation reversal may provide the surviving species with alleles that could be adaptive in deep water (respectively adaptive in a now vacant profundal habitat previously occupied by the recently extinct species). Thus, introgression from the extinct profundal *C. gutturosus* could in principle facilitate adaptation to deep water habitats in some of the surviving Lake Constance whitefish species, that had not occupied these greater depths previously.

Here, we sampled a depth transect on known spawning grounds of *C. macrophthalmus*, the deepest spawning of the extant species. Adaptation to the extinct species' former deep-water habitat seems most plausible in this species. We set nets in six depth zones ranging from 4m to 120m of water depth during spawning season. Thus, we sampled the entire historically known Lake Constance whitefish depth range from that of the shallowest spawning *C. macrophthalmus* populations down to the depths (90-120m) where the extinct *C. gutturosus* used to spawn. We then sequenced whole-genomes of 11 to 17 individuals per depth (total n=96) to search for signatures of differentiation and adaptation along the water depth gradient. We demonstrate that the deepest caught *C. macrophthalmus* individuals from 90m depth show morphological and genetic differentiation from the shallower caught individuals, and we identify 52 candidate loci that might be under positive selection in deep water. At twelve of these loci (23.1%), the allele frequency pattern across our six different spawning depth populations of *C. macrophthalmus* together with the allele frequencies in the historical populations of all Lake Constance whitefish species sampled before speciation reversal (from Frei et al. (2022)) suggest that these alleles might have introgressed from the extinct *C. gutturosus* during the period of anthropogenic lake

eutrophication. Thus, our results demonstrate that some alleles that are likely to have introgressed from the extinct species are potentially involved in adaptation of some populations of *C. macrophthalmus* to the deep-water environment historically used as habitat by the now extinct *C. gutturosus*. This suggests that introgressive hybridization during speciation reversal potentially facilitates adaptation within surviving species to the vacated habitat of a recently extinct species.

Materials and Methods

Study system

In Lake Constance, a large pre-alpine lake bordering Germany, Austria and Switzerland, four whitefish species have been taxonomically described (Steinmann, 1950). *C. wartmanni* is most relevant for commercial fisheries and is extensively managed. It is a pelagic species, mostly feeding on planktonic food resources in the open water (Steinmann, 1950). *C. wartmanni* spawns pelagically, close to the surface over deep water (70-250m) late November until early December (Nenning, 1834; Nüsslin, 1907; Schweizer, 1894; Schweizer, 1926; von Rapp, 1858). *C. macrophthalmus* is the species that is of second largest relevance for commercial fisheries. *C. macrophthalmus* is feeding on both pelagic and benthic food resources (Steinmann, 1950). The species has historically been described to spawn on relatively shallow benthic spawning grounds at depths of less than 20m, close to the shore of the lake, starting from mid-November until early January (Nenning, 1834; Nüsslin, 1907; Eckmann & Rösch, 1998; Schweizer, 1894; Schweizer, 1926; Steinmann, 1950). More recent work suggested an extended range of spawning depth of *C. macrophthalmus* between 2 and 50 meter after the lake has returned to an oligotrophic state (Hirsch, Eckmann, Oppelt, & Behrmann-Godel, 2013; Jacobs et al., 2019). *C. arenicolus* is a relatively large bodied species, feeding on large benthic macroinvertebrates (Steinmann, 1950). It has a very short spawning period mid-November and it has been historically described to spawn on very shallow spawning grounds of 1-2 meters depth and mainly on sandy substrate (Nenning, 1834; Schweizer, 1894; Steinmann, 1950; von Rapp, 1858). *C. gutturosus,* went extinct during the period of anthropogenic eutrophication during the 1970's or 1980's (Vonlanthen et al., 2012). *C. gutturosus* was a deep-water specialist, feeding on benthic macroinvertebrates in the profundal regions of the lake (Steinmann 1950). *C. gutturosus* had an extended spawning

period ranging from summer until winter (Steinmann, 1950), during which it spawned benthically in depths around 70-80m or more (Steinmann, 1950; von Rapp, 1858; von Siebold, 1858).

Sampling

Nets were set at seven different water depths (4m, 12m, 20m, 40m, 60m, 90m and 120m) on a known *C. macrophthalmus* spawning ground at the beginning of the spawning season 2019 (November 26th – November 29th). We used benthic gillnets with varying mesh sizes, consisting of panels of 25mm, 35mm and 45mm mesh size to cover the known range of body sizes of spawning whitefish. We caught fish down to 90m, but not anymore in 120m, suggesting that we covered the whole range of depth that is currently used by whitefish for spawning. Individuals were anaesthetized and subsequently euthanized using appropriate concentrations of tricaine methane sulfonate solutions (MS-222) according to the permit issued by the canton of St.Gallen (SG31396). Fin-clips were taken and stored in 100% analytical ethanol until extraction of DNA. Individual specimens were weighed, total length was measured, a standardized picture was taken and a first species assignment was done on site. All the fish caught were fixed in 4% formalin solution for one month, and then transferred through a series of increasing ethanol concentrations (pure water, 30%, 50%) to the final concentration of 70% for long-term storage.

Morphometric analysis

On all fish caught, we measured 23 linear morphometric traits using digital calliper according to Selz et al. (Selz, Donz, Vonlanthen, & Seehausen, 2020), except for taking the mean of three measurements per trait (instead of the mean of two measurements). The traits measured were BD (body depth), DHL (dorsal head length), PreD (predorsal length), PostD

(postdorsal length), CD (caudal peduncle depth), CL (caudal peduncle length), SL (standard length), HL (head length), HD (head depth), HW (head width), PostO (postorbital length), SN (snout length), ED (eye diameter), EH (eye height), SD (snout depth), SW (snout width), M (length of maxilla), MW (mouth width), UJ (upper jaw length), LJ (lower jaw length), LJW (lower jaw width), IOW (interorbital width), INW (internarial width) (see Table 1 in Selz et al. (2020)). Additionally, we counted the number of gill-rakers (GRC) also according to Selz et al. (Selz et al., 2020). We used individuals that were assigned to *C. macrophthalmus* (n=106) for the following morphological analyses. First, we size corrected our 23 linear morphometric traits by using the residuals of the linear regression of standard length with the specific trait for further analysis. To assess morphological differentiation between fish caught at different depths, we performed a partial least squares regression analysis between all size-corrected traits (excluding standard length and gill-raker count) and depth (4m, 12m, 20m, 40m, 60m, 90m) in R (R Core Team, 2018) using the package "pls" (Mevik & Wehrens, 2007). Finally, we tested whether the first component was significantly correlated with depth using Spearman correlation in R (R Core Team, 2018) to see if morphological differentiation is associated with water depth.

DNA-extraction and sequencing

We sequenced all individuals caught in the 4m, 12m, 40m, 60m, and 90m net. Only for the 20m net, where we caught a total of 31 individuals, we randomly downsampled the number of individuals to 16 to achieve a balanced sampling across all depths. DNA was extracted from fin clips with the Qiagen DNeasy blood and tissue kit (Qiagen AG, CH), using the standard protocol for tissue samples supplied by the manufacturer. DNA concentrations were quantified on a Qubit 2 fluorometer (Thermo Fisher Scientific AG, CH). An Illumina paired-end TruSeq DNA PCR-Free library (Illumina GmbH, CH) was prepared for each fin-

clip sample. Library preparation was performed by the NGS platform of the University of Bern following the manufacturer's instructions. Libraries were then sequenced paired-end 150bp on an Illumina Novaseq 6000 S4 flow cell. Individual sequencing coverage at polymorphic sites (see next section, called across all 91 *C. macrophthalmus* individuals sequenced and with data from at least 85 individuals at each position) was on average ~8.6x and ranged between ~4.3x and ~16.1x in the 91 sequenced *C. macrophthalmus* individuals. Individual coverage did not differ significantly between the different sampling depths according to a one-way ANOVA (p=0.163) performed in R (R Core Team, 2018). Mean coverage was ~8x (range between ~5.6x and ~13.6x) in the 4m spawning depth population, ~7.4x (range between ~4.3x and ~13x) in the 12m spawning depth population, ~8.1x (range between ~4.7x and ~13.9x) in the 20m spawning depth population, ~10.4x (range between ~6.2x and ~16.1x) in the 40m spawning depth population, ~10x (range between ~5x and ~14.8x) in the 60m spawning depth population, and ~8.1x (range between ~5.1x and ~14.1x) in the 90m spawning depth population.

Processing reads and mapping

Raw reads were processed and mapped to the Alpine whitefish reference genome following Frei et al. (2022). In brief, poly-G tails were removed using fastp 0.20.0 (Chen, Zhou, Chen, & Gu, 2018) and overlapping read pairs with overlaps longer than 25bp were subsequently merged using Seqprep 1.0 (https://github.com/jstjohn/SeqPrep). The processed reads were then mapped to Alpine whitefish reference genome (De-Kayne, Zoller, & Feulner, 2020) using BWA 0.7.12 (Li & Durbin, 2009) adjusting the "r" parameter to 1. We marked duplicate reads, fixed mate information and replaced read groups (settings used except for the default parameters were VALIDATION_STRINGENCY=LENIENT and MAX_FILE_HANDLES_FOR_READ_ENDS_MAP=1024) using picard tools 2.20.2

(http://broadinstitute.github.io/picard/).

Population genomic analysis

We then used angsd version 0.925 (Korneliussen, Albrechtsen, & Nielsen, 2014) to calculate genotype likelihoods across all 96 samples caught at the 6 different depths, and additionally included all historical individuals of Frei et al. (2022) (short read archive accession number PRJEB43605) to verify species assignment that was done in the field. Only sites covered with at least two reads in at least 118 individuals (out of a total of 128 individuals) and passing a p-value cut-off of 10E-6 for being variable were included, while all sites with more than two alleles were excluded. Reads that did not map uniquely to the reference and had a mapping quality below 30, as well as bases with quality score below 20 were not considered. The following p-value cut-offs for SNP filters implemented in angsd version 0.925 (Korneliussen et al., 2014) were used: -sb_pval 0.05 -qscore_pval 0.05 -edge_pval 0.05 -mapq_pval 0.05. To verify species assignment based on the resulting 941'976 SNPs with minor allele frequency above 0.05 (default parameter of PCAngsd 0.98), we did a PCA and calculated admixture proportions based on the thirst three eigenvectors (-e 3) using PCAngsd 0.98 (Meisner & Albrechtsen, 2018). In total, we identified one individual to belonging to *C. wartmanni* (or possibly being early generation hybrids) and four individuals belonging to *C. arenicolus* (matching our species assignment done in the field) and thus these five samples have been excluded from subsequent analysis. We used a generalized linear model (glm) in R (R Core Team, 2018) to test whether the *C. gutturosus* admixture proportions were different between the different depths that we sampled.

We then used eleven *C. gutturosus* individuals and the two historical *C. macrophthalmus* individuals from Frei et al. (2022) in combinations with the 91 *C. macrophthalmus* individuals caught at either 4m, 12m, 20m, 40m, 60m, or 90m to test for

introgression from *C. gutturosus* into each spawning depth population separately, using the population-based D-statistics (Soraggi, Wiuf, & Albrechtsen, 2018) implemented in angsd 0.925 (Korneliussen et al., 2014). We first calculated genotype likelihoods using only the 104 above mentioned samples and using the same parameters as described above but adjusting the missing data parameter to include sites with data from at least 99 individuals. This resulted in a total of 517'250 SNPs that were then used for the D-statistics. We used a *S. salar* individual from Kjaerner-Semb et al. (Kjaerner-Semb et al., 2016) (short read archive accession number: SSR3669756) as outgroup P4, the eleven *C. gutturosus* individuals as donor population P3, all *C. macrophthalmus* individuals of one of the six sampled depths as P2 and the two historical *C. macrophthalmus* as P1. By that ordering of populations on the four-taxon topology, it is possible to test for excess allele sharing between *C. gutturosus* and post-eutrophication populations of extant species relative to the same species sampled pre-eutrophication, which would be indicative of introgression of *C. gutturosus* into this species during eutrophication. We then repeated the analysis but replaced the donor population P3 with all historical *C. arenicolus* and *C. wartmanni* individuals from Frei et al. (2022) to test for introgression of *C. arenicolus* or *C. wartmanni* respectively into our six *C. macrophthalmus* spawning depth populations that must have happened during eutrophication-induced speciation reversal.

We then calculated genotype likelihoods again, using the same parameters as above but only using the 91 *C. macrophthalmus* samples and adjusting the missing data parameter to include sites where data for at least 85 individuals was available. We used the resulting genotype likelihoods at 1'948'989 polymorphic sites to calculate (weighted) F_{ST} (Bhatia, Patterson, Sankararaman, & Price, 2013) between all possible pairs of spawning depth populations (as well as between 90m and all other spawning depth populations pooled) in angsd 0.925 (Korneliussen et al., 2014) based on one- and two-dimensional site frequency

spectra inferred from site allele frequencies (Nielsen, Korneliussen, Albrechtsen, Li, & Wang, 2012). We then again calculated a PCA with PCAngsd (0.98) (Meisner & Albrechtsen, 2018) at the 1'126'828 SNPs with minor allele frequency above 0.05 (default parameter of PCAngsd 0.98) to visualize population structure across depth within *C. macrophthalmus*. We further performed a selection scan along PC1 using PCAngsd (0.98) (Meisner & Albrechtsen, 2018) according to the method proposed by Galinksy et al. (2016). The method identifies unusual allele frequency shifts along previously inferred PC-axes, making use of the fact that the squared correlation of each SNP to a specific PC-axis, rescaled to account for genetic drift, follows a chi-square distribution (1 d.o.f) under the null hypothesis of the absence of selection (Galinsky et al., 2016). As PC1 separated the fish caught at 90m from all the fish caught shallower (4m, 12m, 20m, 40m, 60m), this selection scan would detect positions that are under selection in deep-water, respectively involved in depth adaptation. Following Pinsky et al. (2021), we FDR-corrected the resulting P-values and assumed SNPs with an FDR-corrected P-value below 0.05 to be under selection. P-values were then log transformed for plotting using R (R Core Team, 2018).

At the 107 SNPs above the FDR-corrected significance threshold from the PCA-based selection scan, we used angsd 0.925 (Korneliussen et al., 2014) to calculate allele frequencies from genotype likelihoods of each spawning depth population separately using the method described in Kim et al. (2011), and we fixed the tracked allele to represent the reference allele of the Alpine whitefish reference genome. To remove redundant sites in strong physical linkage, we only considered positions that are more than 5 Mbp apart from each other. We retained 52 SNPs for further analysis. We then additionally calculated the allele frequency in all historical *C. gutturosus* (n=11) individuals, as well as in all historical *C. macrophthalmus* (n=2), *C. arenicolus* (n=3) and *C. wartmanni* (n=2) individuals from Frei et al. (2022). SNPs that have a minor allele frequency above 0.05 in *C. gutturosus*, but are absent from all

historical *C. macrophthalmus*, *C. arenicolus and C. wartmanni* have potentially been characteristic for *C. gutturosus* before the eutrophication period. Considering that our data showed that there was significant *C. gutturosus* introgression, detecting an allele with such a frequency pattern in contemporary populations of the extant species suggests that this allele introgressed from *C. gutturosus* during the anthropogenic eutrophication period. Following this logic, we looked for SNPs with such an allele frequency pattern consistent with *C. gutturosus* introgression among the 52 independent SNPs inferred to be under selection between deep and shallower spawning *C. macrophthalmus* to find SNPs with alleles that potentially introgressed from *C. gutturosus* that may now facilitate deep-water adaptation in deep spawning *C. macrophthalmus*. We tested by permutation if the 52 sites potentially under selection between deep and shallower caught *C. macrophthalmus* are significantly enriched for SNPs with an allele frequency pattern consistent with *C. gutturosus* introgression. We randomly subsampled 52 positions (the same number as inferred to be under selection between deep and shallower spawning *C. macrophthalmus*), and then calculated the proportion of these subsampled SNPs that show an allele frequency pattern consistent with *C. gutturosus* introgression. We repeated this random subsampling 10'000 times to generate a null expectation, and then calculated a P-value by comparing the expected proportion of sites showing an allele frequency pattern of *C. gutturosus* introgression of these 10,000 permutations with the observed proportion calculated within the 52 sites potentially under selection between deep and shallower spawning *C. macrophthalmus*.

Finally, we assessed if the 107 SNPs (in 52 independent genomic regions) inferred to be under selection fall within genes, and if yes, in which genes. Gene annotations (from the Alpine whitefish genome (De-Kayne et al., 2020); ENA accession: GCA_902810595.1) that overlap with the loci potentially under selection were identified using bedtools v.2.28.0 (Quinlan, 2014). We then used the protein sequence of the overlapping gene from the Alpine

whitefish genome (De-Kayne et al., 2020; ENA accession: GCA_902810595.1) to perform a protein-protein BLAST (blastp) search against all genes of the annotation of the *S. salar* genome (taxid 8030). We reported the best hit for each gene (Supplementary Table 4).

Results

Sampling populations of *C. macrophthalmus* along a spawning depth gradient

We sampled the entire known spawning depth range of *C. macrophthalmus* (4m, 12m, 20m, 40m), as well as greater depths where the extinct *C. gutturosus* used to spawn (60m, 90m, 120m) during the *C. macrophthalmus* spawning season end of November 2019 (see Figure 1A). Our sampling timepoint was in the middle of the typical spawning season of the targeted *C. macrophthalmus* (early November until early January), but also overlapped the spawning season reported for the now extinct *C. gutturosus*, ranging from July to early January (Steinmann, 1950). In total, we caught 106 *C. macrophthalmus* individuals, of which 93 (~88%) were fully ripe. While most fish were caught at 20m (n=31, Figure 1B), we caught spawning *C. macrophthalmus* individuals down to 90m, but no fish were caught at the greatest depth fished (120m). This suggests that our sampling covered the entire range of depth that is currently used for spawning by whitefish.

To verify our species assignment that was done in the field, we performed a genomic principal component analysis (PCA; Supplementary Figure 1) and a structure analysis (Supplementary Figure 2) using genotype likelihoods of 941'976 SNPs. We included all 96 sequenced individuals, as well as historical and contemporary individuals used in Frei et al. (2022) for reference. In both genomic PCA and structure analysis (Supplementary Figures 1 and 2), four individuals of a total of 96 turned out to belong to *C. arenicolus*, and thus were subsequently excluded from further analysis. One individual caught at 90m clustered with *C. wartmanni* in the PCA and looked like an early generation hybrid in the structure analysis. This fish was also excluded from all subsequent analyses to ensure that the results reflect solely the variation within *C. macrophthalmus* (n=91).

Morphological and genomic differentiation along the spawning depth gradient

We performed a partial least squares regression analysis based on linear morphometric measurements of 23 body- and head traits (size corrected by using residuals of linear regression against standard length) against spawning depth on all 106 individuals assigned to *C. macrophthalmus* (91 individuals randomly selected for sequencing, plus the 15 individuals that were caught but not sequenced). We found indications for morphological differentiation along depth (Figure 1D), with component 1 being significantly correlated with depth (rho=-0.44, p=2e-06, Supplementary Figure 3). The traits with the highest loadings on both component 1 (LJW=0.70, SD=0.69 and MW=0.39) and component 2 (SW=-0.55, EH=-0.49 and SNL=-0.35) were related to mouth (and head) shape (Supplementary Figure 4). In contrast, our analysis of the genomic data did not yield any evidence for genomic differentiation along the spawning depth gradient when genome-wide F_{ST} was used as test metric. We performed a genomic PCA based on genotype-likelihoods of 1'126'828 SNPSs in all sequenced individuals genetically assigned to *C. macrophthalmus* (n=91; out of a total of 96 individuals that were randomly selected for sequencing). We found that the principal component explaining most variation (PC1, Figure 1C) separates the deepest caught individuals (90m) from all others, but the genome-wide F_{ST} between the 90m sample and all shallower caught individuals did not differ from zero (weighted F_{ST}= -0.001567; all pairwise genome-wide F_{ST}'s between depth categories were below zero). Similar to the morphological results, genomic PC1 was significantly correlated with depth (rho=-0.37, p=0.0003, Supplementary Figure 3). Taken together, our high-resolution data allows to identify subtle intra-specific differentiation within *C. macrophthalmus* in both genomic and morphological data (Figure 1C and Figure 1D). The correlation of both morphological and genomic variation with depth suggests that the observed differentiation may be related to the onset of adaptation to deep-water. Even though we did not observe genome-wide differentiation based on

genome-wide F_{ST} estimates which reflect neutral demographic processes that affect all SNPs (as the majority of SNPs along the genome are expected to evolve neutrally), our PCA approach demonstrates intraspecific differentiation within *C. macrophthalmus* between fish spawning at 90m and all shallower spawning individuals. However, this pattern might be driven by relatively few loci, which potentially show differentiation in consequence of selective processes.

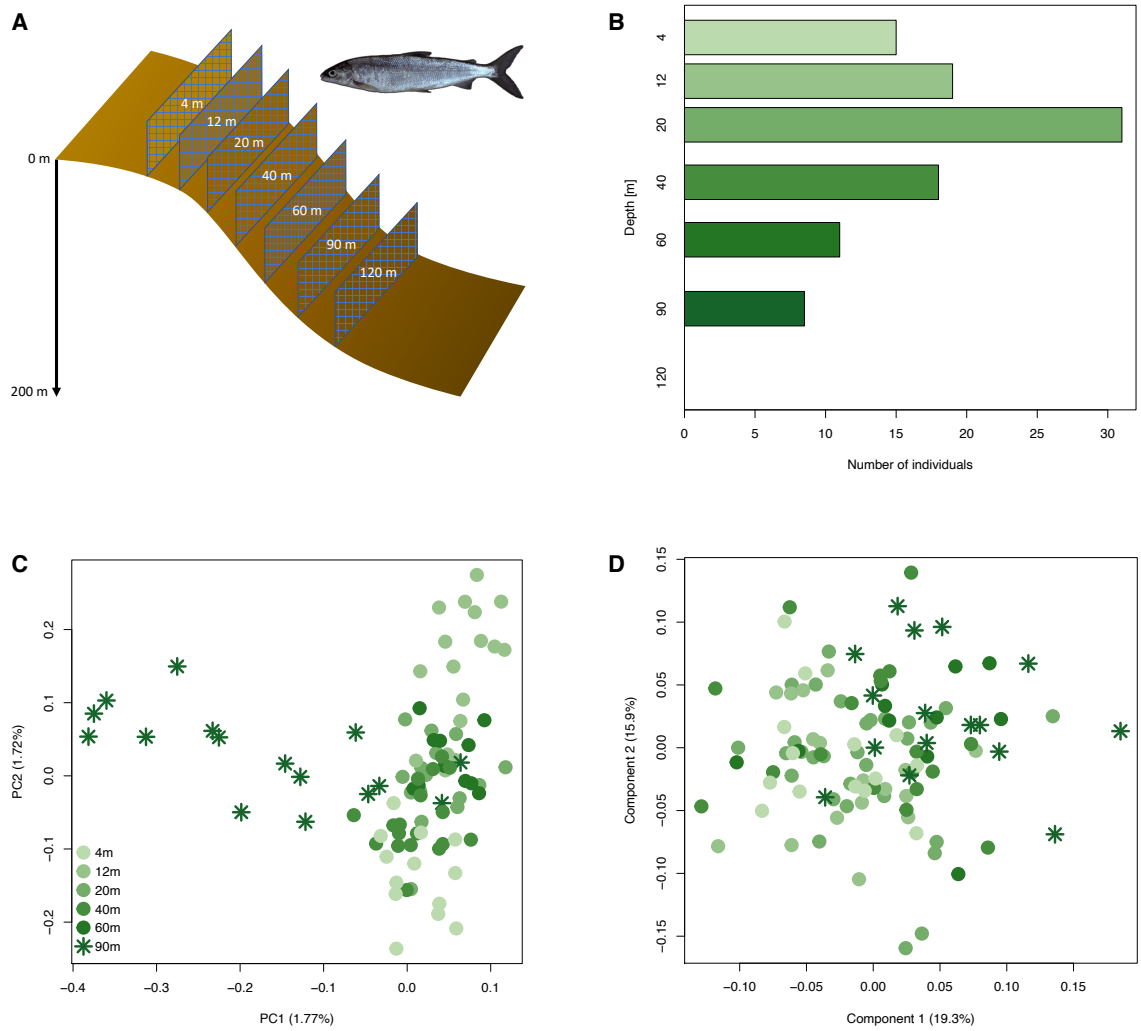

Figure 1: Differentiation along a water depth gradient. A) Schematic overview of the sampling structure with nets set at seven different depths. **B)** Number of individuals caught at each depth within 18h (same sampling effort for each depth). **C**) Genomic variation based on 1'126'828 polymorphic sites illustrated by a principal component analysis (PCA). The depth category of each individual is indicated by different green shadings (the deeper the darker). The 90m spawning depth population is highlighted with asterisks, while all other spawning depth populations are indicated by dots. **D**) Morphological differentiation is displayed as the two major components resulting from the partial least squares regression analysis. Symbols and colours are the same as in Figure 1C.

Introgression from extinct deep-water species

We tested whether the six different *C. macrophthalmus* spawning depth populations (n=11-16) received significant introgression from either *C. gutturosus*, *C. arenicolus* and/or *C wartmanni*, by making use of the historical samples of Frei et al (2022). We detected significant introgression from *C. gutturosus* and *C. wartmanni* into each of our six *C. macrophthalmus* spawning depth populations (n=11-16; Supplementary Table 1 and 2), but we did not detect significant introgression from *C. arenicolus* (Supplementary Table 3). Per-individual *C. gutturosus* admixture proportions were not different between different depths (see Figure 2; p=0.616 in a generalized linear model). However, the variance in admixture proportion was highest in the two deepest nets (60 and 90m) and the individual with the highest admixture proportion (~14%) was caught at 60m.

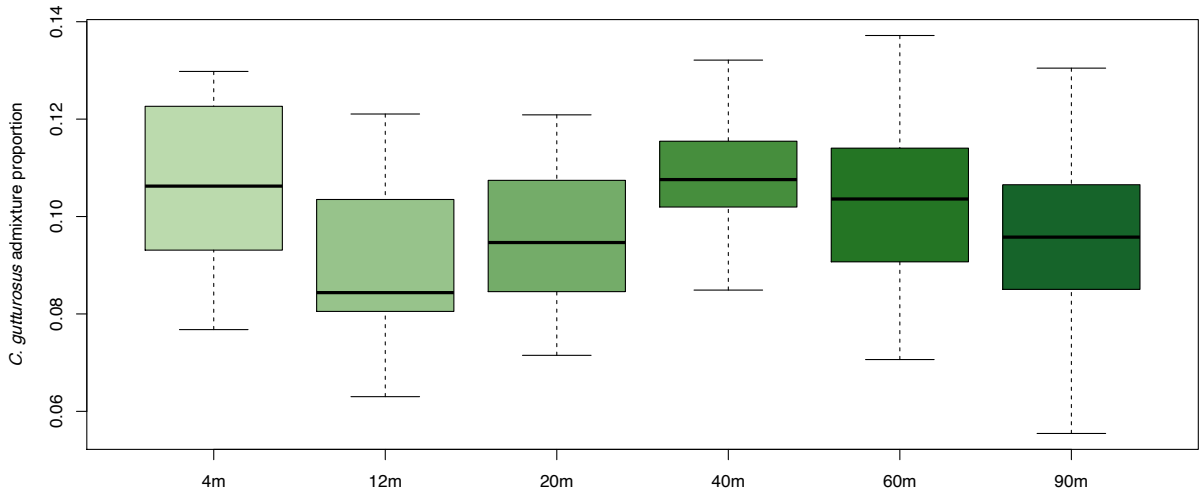

Figure 2: No differences in admixture proportions between spawning depth populations. Boxplots showing the *C. gutturosus* admixture proportions from the PCAngsd admixture analysis (see Supplementary Figure 2) in each spawning depth population. Horizontal bars correspond to medians, and whiskers to 1.5 times the interquantile range. There were no significant differences in admixture proportions between spawning depth populations (p=0.616 in a generalized linear model).

Identifying genomic positions shaped by selection along the water depth gradient

We performed the selection scan proposed by Galinsky et al. (Galinsky et al., 2016) implemented in PCAngsd (Meisner & Albrechtsen, 2018; Meisner, Albrechtsen, & Hanghoj, 2021) to find positions under selection between the *C. macrophthalmus* spawning depth populations. The method works best with data that is continuously distributed in PC-space (Galinsky et al., 2016; Meisner & Albrechtsen, 2018) (see Figure 1C) and identifies positions that significantly deviate from genetic drift along an axis of differentiation (Meisner et al., 2021). As our PC1 (see Figure 1) is separating most of the 90m *C. macrophthalmus* from all samples from shallower depths, positions that are detected to be under selection along this PC-axis would thus potentially be involved in adaptation to deep water. In total, we found 107 outlier SNPs (FDR-corrected p<0.05) in 52 independent genomic regions (at least 5 Mbp apart from each other) that are potentially under selection between the 90m spawning site and shallower sites (Figure 3A). These 107 outlier SNPs overlapped a total of 30 genes (see Supplementary Table 4).

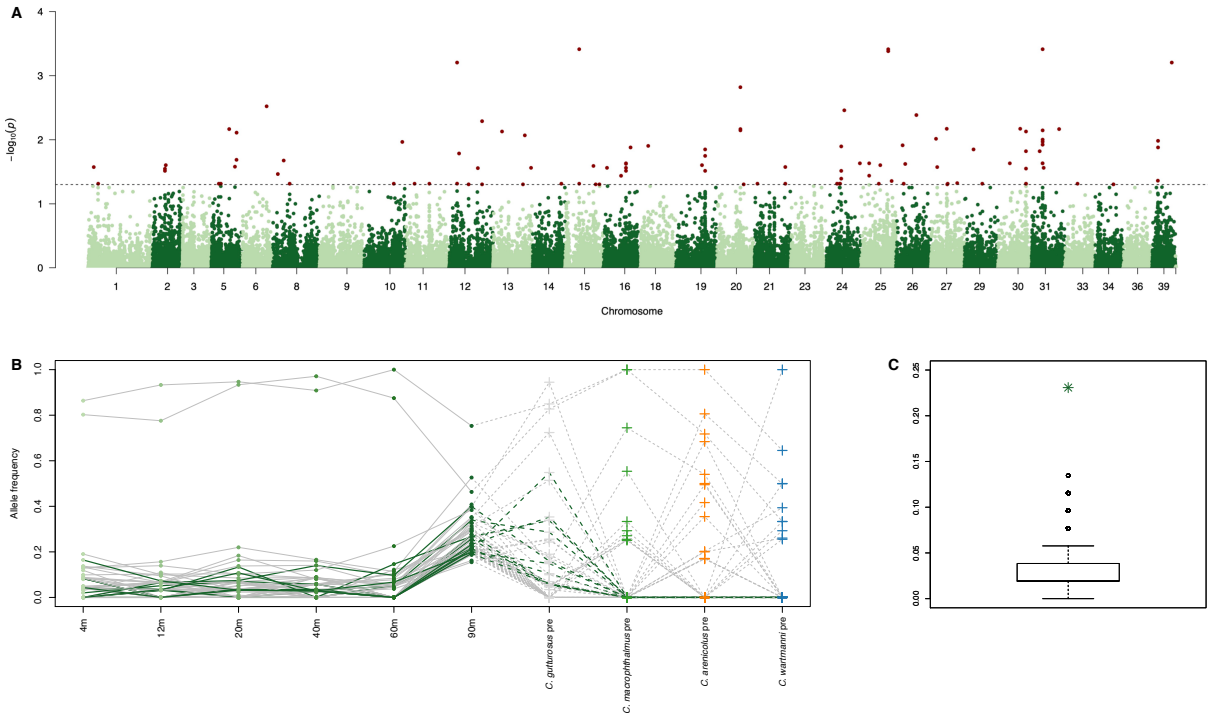

Figure 3: *C. gutturosus* introgression is enriched at positions under selection between shallow and deep water. A) Selection scan along PC1 from our genomic PCA (see Figure 1C) from Galinksy et al. (2016) as implemented in PCAngsd (Meisner & Albrechtsen, 2018; Meisner et al., 2021). As PC1 separates the 90m population from shallower spawning *C.*

macrophthalmus populations, this approach identifies positions potentially under selection between deep and shallow spawning individuals. Shown are log-transformed and FDR-corrected p-values. The dashed line indicates the FDR-corrected 0.05 significance threshold, and all positions with p-values below the threshold are coloured in darkred. **B)** Allele frequencies in the six different spawning depth populations (4-90m) and in historical populations from Frei et. al (2022) (indicated with crosses and denoted with "pre"; grey for *C. gutturosus* (n=11), green for *C. macrophthalmus* (n=2), orange for *C. arenicolus* (n=3) and blue for *C. wartmanni* (n=2)). Shown are the 52 positions with an FDR-corrected p-value below 0.05 and at least 5 Mbp apart from each other. SNPs derived from *C. gutturosus* and potentially introgressed into *C. macrophthalmus* during eutrophication (frequency in *C. gutturosus* above 0.05, but allele is absent from all other historical populations) are coloured in green. **C**) The distribution of 10'000 permutations of 52 randomly sampled positions (same number as shown in Figure 2B) along the genome, showing the proportion of alleles derived from *C. gutturosus* and potentially introgressed into *C. macrophthalmus* during eutrophication (same pattern as dark green trajectories in B). The green asterisk indicates the observed value (the 12 out of 52 in B).

Allele frequency patterns consistent with introgression from extinct deep-water species

To assess whether adaptation to deep water in *C. macrophthalmus* was potentially facilitated by alleles introgressed from *C. gutturosus*, we assessed the population allele frequency in our six spawning depth populations (4m, 12m, 20m, 40m, 60m and 90m) at the 52 independent genomic positions with evidence for selection between the deepest (90m) and all shallower (4-60m) spawning *C. macrophthalmus* populations. Additionally, we also inferred allele frequencies at the same positions in 11 historical *C. gutturosus* individuals, two historical *C. macrophthalmus* individuals, three historical *C. arenicolus* individuals and two historical *C. wartmanni* individuals sampled from before the onset of eutrophication from Frei et al (2022). At 12 out of 52 (23.1%) positions under selection between deep and shallower spawning *C. macrophthalmus*, we found that the alternate allele was present in *C. gutturosus* before the eutrophication period, while the allele was absent in the historical *C. macrophthalmus*, *C. arenicolus* and *C. wartmanni* samples from Frei et al. (2022) (Figure 3B). This pattern of allele frequencies across populations and species suggests that these alleles, potentially involved in adaptation to deep water in *C. macrophthalmus*, likely introgressed from *C. gutturosus* during the anthropogenic eutrophication period. Sites with

such an allele frequency pattern consistent with *C. gutturosus* introgression were significantly enriched among the 52 independent sites that are potentially under selection between deep and shallower caught *C. macrophthalmus* ($p<10e-4$ obtained with 10'000 permutations, Figure 3C), suggesting that introgressed alleles from *C. gutturosus* may facilitate adaptation to deep water in *C. macrophthalmus*.

Discussion

Anthropogenic eutrophication of Lake Constance during the last century resulted in the extinction of the endemic profundal whitefish species *Coregonus gutturosus*, caused by a combination of demographic decline and speciation reversal through introgressive hybridization with other species of the same radiation. Introgression during speciation reversal resulted in the persistence of considerable parts of genomic variation from the extinct species within several extant species (Frei et al., 2022). We here show that one of the surviving Lake Constance whitefish species, *C. macrophthalmus*, is currently re-populating the deep-water environment that was left vacated after the extinction of *C. gutturosus.* Our systematic sampling of a spawning depth gradient demonstrated that today, *C. macrophthalmus* is spawning in greater depths (down to 90m) than previously reported for this species (less than ~20m before eutrophication in e.g., Nüsslin (1907) and Schweizer (1926), or ~20m in Eckmann & Rösch (1998) and 2-50m in Jacobs et al. (2019) after eutrophication). Our data suggests that introgression from *C. gutturosus* that occurred during its decline, potentially facilitates ongoing adaptation to the vacated deep-water niche in *C. macrophthalmus*.

Re-population of and adaptation to the vacated deep-water environment

Adaptation to deep water conditions at the lower end of a species' depth range is expected to result in morphological and genomically localized rather than genome-wide differentiation between populations spawning deep and those that spawn shallower, as selection is thought to favour phenotypes or combinations of alleles that increase fitness in deep-water habitats. Founder effects during range expansion might mimic adaptation, and hence could be mistaken for signals of adaptation. However, a founder effect would require

some degree of geographical isolation between founder and source populations. As *C. macrophthalmus* has expanded its ecological niche at a spatial scale that lies within the dispersal distance of a single individual, a founder effect in the 90m spawning depth population is unlikely. Furthermore, a founder effect in the deepest spawning population should be associated with an increase of genetic drift due to reduced effective population size. As a consequence, genetic diversity would decrease, resulting in genome-wide differentiation to all other spawning depth populations. In contrast with this prediction, we did not find evidence for genomic differentiation measured with genome-wide F_{ST}, which would reflect genome-wide differentiation resulting from demographic processes. Our data provides evidence for both subtle morphological and genomic differentiation between the deepest-spawning (90m) and shallower (4-60m) spawning populations of *C. macrophthalmus*. This subtle genomic differentiation might be genomically localized rather than genome-wide, considering the evidence for differentiation between the 90m spawning depth population in the PCA (see Figure 1C), but no evidence for such differentiation when using genome-wide F_{ST}. Additionally, the major axis of genomic differentiation and of morphological differentiation were both correlated with spawning depth. This suggests that the observed intraspecific differentiation between the 90m spawning depth population and all shallower spawning depth populations might indeed be a result of adaptation to the vacant deep-water niche.

Until recently, whitefish have been reported absent from deep-water habitats of Lake Constance (Alexander & Seehausen, 2021). Thus, the colonization of and adaptation to deep water in *C. macrophthalmus* described here has likely started only recently. This is consistent with theoretical work that demonstrated that, when a species goes extinct through hybridization, the re-population of its habitat is likely when disturbance that led to reversal is of only short duration (Gilman & Behm, 2011). Hybridization during the extinction process

facilitates the re-emergence of a similar phenotype to that of the extinct species through a combination of alleles derived from surviving and the extinct species, finally enabling the re-population of the vacated habitat. Adaptation and diversification by re-assembling alleles from two hybridizing species into new adaptive trait combinations is thought to be orders of magnitudes faster than adaptation and speciation based on *de-novo* mutation alone (Marques et al., 2019), and thus might be an important process in rapid adaptation to changing environments.

Introgression facilitates adaption to extinct species' habitat

Introgression from *C. gutturosus* during eutrophication-induced speciation reversal might have provided the contemporary *C. macrophthalmus* population with alleles that are adaptive in deep water. The significant introgression from *C. gutturosus* into *C. macrophthalmus* caught in any depth zone demonstrated by D-statistics in combination with the matching allele frequencies between *C. gutturosus* and our 90m *C. macrophthalmus* sample suggests that parts of the adaptation to deep water in *C. macrophthalmus* could be based on selection on introgressed variation derived from *C. gutturosus*. Ecological selection on introgressed variation is predicted to result in biased ancestry around functionally relevant genomic regions (Moran et al., 2021). However, as both positive and negative selection may act on genomic variation derived from introgression (as for example demonstrated for Neanderthal introgression into some populations of *Homo sapiens*; see e.g., Huerta-Sanchez et al. (2014), Racimo, Sankararaman, Nielsen, & Huerta-Sanchez (2015), Reilly et al. (2022) and Harris & Nielsen (2016)), determining the exact selective forces acting on a specific allele is complex and challenging (Moran et al., 2021). At twelve out of 52 independent positions (23.1%) indicating signatures of positive selection (and thus potentially involved in adaptation to depth), the patterns of allele frequencies suggested that the allele with increased

frequency in the 90m spawning depth population might have introgressed from *C. gutturosus*. Even though the sample sizes for the historical populations of the three extant species is limited, our permutation approach demonstrates that alleles that likely introgressed from *C. gutturosus* are enriched at positions under divergent selection between the deepest (90m) and shallower spawning (4-60m) *C. macrophthalmus* populations. This suggests that introgression from the extinct *C. gutturosus* might facilitate adaptation to its former deep-water habitat in the extant *C. macrophthalmus*. These results are in line with recent work that demonstrated that adaptation based on variation derived from recent admixture events can be very rapid and take only few generations (Hamid et al., 2021). Further, our findings are consistent with the syngameon hypothesis of adaptive radiations, predicting that hybridization between species within an adaptive radiation can promote further diversification and speciation (Seehausen, 2004). Especially when environments change, hybridization within an adaptive radiation might increase the genomic variation of individual species and thereby enhance their adaptive potential, enabling a faster evolutionary response to the novel selective pressures of a changing environment (Grant & Grant, 2019). Consequently, hybridization between members of an adaptive radiation might be especially relevant under environmental change, potentially facilitating the survival of several species or even all species in a radiation through elevated evolvability and faster adaptation to the changing environmental conditions.

Ecological recovery through evolution

Anthropogenic environmental change is affecting ecosystems worldwide whilst a large portion of contemporary species diversity is sensitive to hybridization-driven dynamics (Grabenstein & Taylor, 2018). Thus, the potential for speciation reversal to affect evolutionary trajectories of species and lineages is enormous (Seehausen et al., 2008). Our results suggest that the colonization of a vacated niche could potentially occur on a short

evolutionary time-scale when adaptation of an extant species is facilitated by introgression of alleles from the species that occupied this niche in the past and now is extinct. Such introgressed alleles have already been tested by selection in the environment originally inhabited by the extinct species. These alleles likely have the potential to facilitate rapid adaptation of the recipient species to these environmental conditions, provided that the disturbance resulting in extinction through speciation reversal was transient and of short duration (Gilman & Behm, 2011). This highlights the importance of quick and efficient ecosystem restorations after anthropogenic disturbances to maximize the chance of ecological recovery through evolution.

Hybridization in response to homogenized environments can result in dramatic losses of biodiversity within few generations (Taylor et al., 2006; Grabenstein & Taylor, 2018). However, hybridization can as well facilitate adaptation when environments become more heterogeneous again and thus promote the evolution of new biodiversity (Moran et al., 2021). When alleles that have evolved in a now extinct species introgress into a surviving species, they can outlast the species they evolved in and potentially be re-used to adapt to the extinct species' vacated habitat, other habitats, or changed environmental conditions. The role of hybrid populations has been controversial in conservation biology (Draper, Laguna, & Marques, 2021). However, hybrid populations with high genetic variation and in turn high evolvability, such as those resulting from speciation reversal, can be important for future evolutionary dynamics that could contribute to the ecological recovery of an ecosystem. In turn, efficient and informed conservation measures should consider the implications of the existence of such hybrid populations with high adaptive potential and the evolutionary dynamics that can emerge from them, potentially contributing to the recovery of an ecosystem on a time-scale that is much shorter than the usually assumed evolutionary timescales of millenia.

Acknowledgements

We thank Christoph Birrer, Michael Kugler and Jörg Schweizer from the Amt für Natur, Jagd und Fischerei, St.Gallen and we are very thankful for their valuable information and support during planning and sampling. We want to thank Carmela Dönz, Marta Reyes, Oliver Selz and Lukas Aerne for help during fieldwork and Andres Grolimund for measuring linear morphometric traits and counting gill-rakers. We thank the NGS facility of the University of Bern for sequencing support and the genetic diversity center (GDC) at ETH Zurich for bioinformatic support. This work received financial support from Eawag (including Eawag Discretionary Funds 2018-2022) and the Swiss Federal Office for the Environment. The work was further supported by the grant "SeeWandel: Life in Lake Constance – the past, present and future" within the framework of the Interreg V programme "Alpenrhein-Bodensee-Hochrhein (Germany/Austria/Switzerland/Liechtenstein)" which funds are provided by the European Regional Development Fund as well as the Swiss Confederation and cantons (to P.F. and O.S.). The funders had no role in study design, decision to publish, or preparation of the manuscript.

References

Alexander, T., & Seehausen, O. (2021). *Diversity, distribution and community composition of fish in perialpine lakes - "Projet Lac" synthesis report*. Bern: 2021.

Barlow, A., Cahill, J. A., Hartmann, S., Theunert, C., Xenikoudakis, G., Gonzalez Fortes, G., . . . Hofreiter, M. (2018). Partial genomic survival of cave bears in living brown bears. *Nature Ecology & Evolution, 2*(10), 1563-1570. doi:10.1038/s41559-018-0654-8

Bhatia, G., Patterson, N., Sankararaman, S., & Price, A. L. (2013). Estimating and interpreting F_{ST}: The impact of rare variants. *Genome Research, 23*(9), 1514-1521. doi:10.1101/gr.154831.113

Chen, S. F., Zhou, Y. Q., Chen, Y. R., & Gu, J. (2018). Fastp: an ultra-fast all-in-one FASTQ preprocessor. *Bioinformatics, 34*(17), 884-890. doi:10.1093/bioinformatics/bty560

De-Kayne, R., Zoller, S., & Feulner, P. G. D. (2020). A de novo chromosome-level genome assembly of *Coregonus sp.* "Balchen": One representative of the Swiss Alpine whitefish radiation. *Molecular Ecology Resources, 20*(4), 1093-1109. doi:10.1111/1755-0998.13187

Deufel, J., Löffler, H., & Wagner, B. (1986). Auswirkungen der Eutrophierung und anderer anthropogener Einflüsse auf die Laichplätze einiger Bodensee-Fischarten. *Österreichs Fischerei, 39*, 325-336.

628 Draper, D., Laguna, E., & Marques, I. (2021). Demystifying negative connotations of
629 hybridization for less biased conservation policies. *Frontiers in Ecology and*
630 *Evolution, 9*(637100). doi:10.3389/fevo.2021.637100

631 Eckmann, R., & Rösch, R. (1998). Lake Constance fisheries and fish ecology. *Advances in*
632 *Limnology, 53*, 285-301.

633 Frei, D., De-Kayne, R., Selz, O. M., Seehausen, O., & Feulner, P. G. D. (2022). Genomic
634 variation from an extinct species is retained in the extant radiation following
635 speciation reversal. *Nature Ecology & Evolution,* 6(4), 461-468. doi:10.1038/s41559-
636 022-01665-7

637 Galinsky, K. J., Bhatia, G., Loh, P. R., Georgiev, S., Mukherjee, S., Patterson, N. J., & Price,
638 A. L. (2016). Fast principal-component analysis reveals convergent evolution of
639 ADH1B in Europe and East Asia. *American Journal of Human Genetics, 98*(3), 456-
640 472. doi:10.1016/j.ajhg.2015.12.022

641 Gilman, R. T., & Behm, J. E. (2011). Hybridization, species collapse, and species
642 reemergence after disturbance to premating mechanisms of reproductive isolation.
643 *Evolution, 65*(9), 2592-2605. doi:10.1111/j.1558-5646.2011.01320.x

644 Grabenstein, K. C., & Taylor, S. A. (2018). Breaking barriers: causes, consequences, and
645 experimental utility of human-mediated hybridization. *Trends in Ecology & Evolution,*
646 *33*(3), 198-212. doi:10.1016/j.tree.2017.12.008

647 Grant, P. R., & Grant, B. R. (2019). Hybridization increases population variation during
648 adaptive radiation. *Proceedings of the National Academy of Sciences of the United*
649 *States of America, 116*(46), 23216-23224. doi:10.1073/pnas.1913534116

650 Hamid, I., Korunes, K. L., Beleza, S., & Goldberg, A. (2021). Rapid adaptation to malaria
651 facilitated by admixture in the human population of Cabo Verde. *Elife, 10*.
652 doi:10.7554/eLife.63177

653 Harris, K., & Nielsen, R. (2016). The genetic cost of Neanderthal introgression. *Genetics,*
654 *203*(2), 881-891. doi:10.1534/genetics.116.186890

655 Hirsch, P. E., Eckmann, R., Oppelt, C., & Behrmann-Godel, J. (2013). Phenotypic and
656 genetic divergence within a single whitefish form - detecting the potential for future
657 divergence. *Evolutionary Applications, 6*(8), 1119-1132. doi:10.1111/eva.12087

658 Hudson, A. G., Lundsgaard-Hansen, B., Lucek, K., Vonlanthen, P., & Seehausen, O. (2016).
659 Managing cryptic biodiversity: Fine-scale intralacustrine speciation along a benthic
660 gradient in Alpine whitefish (Coregonus spp.). *Evolutionary Applications*, *10*, 251-
661 266. doi:10.1111/eva.12446

662 Huerta-Sanchez, E., Jin, X., Asan, Bianba, Z., Peter, B. M., Vinckenbosch, N., . . . Nielsen, R.
663 (2014). Altitude adaptation in Tibetans caused by introgression of Denisovan-like
664 DNA. *Nature, 512*(7513), 194-197. doi:10.1038/nature13408

665 Ingram, T., Hudson, A. G., Vonlanthen, P., & Seehausen, O. (2012). Does water depth or diet
666 divergence predict progress towards ecological speciation in whitefish radiations?.
667 *Evolutionary Ecology Research, 14*(4), 487-502. doi:10.7892/boris.16333

668 Irisarri, I., Singh, P., Koblmuller, S., Torres-Dowdall, J., Henning, F., Franchini, P., . . .
669 Meyer, A. (2018). Phylogenomics uncovers early hybridization and adaptive loci
670 shaping the radiation of Lake Tanganyika cichlid fishes. *Nature Communications,*
671 *9*(3159). doi:10.1038/s41467-018-05479-9

672 Jacobs, A., Carruthers, M., Eckmann, R., Yohannes, E., Adams, C. E., Behrmann-Godel, J.,
673 & Elmer, K. R. (2019). Rapid niche expansion by selection on functional genomic
674 variation after ecosystem recovery. *Nature Ecology & Evolution, 3*(1), 77-86.
675 doi:10.1038/s41559-018-0742-9

676 Kim, S. Y., Lohmueller, K. E., Albrechtsen, A., Li, Y. R., Korneliussen, T., Tian, G., . . .
677 Nielsen, R. (2011). Estimation of allele frequency and association mapping using
678 next-generation sequencing data. *Bmc Bioinformatics, 12*(231). doi:10.1186/1471-
679 2105-12-231

680 Kjaerner-Semb, E., Ayllon, F., Furmanek, T., Wennevik, V., Dahle, G., Niemela, E., . . .
681 Edvardsen, R. B. (2016). Atlantic salmon populations reveal adaptive divergence of
682 immune related genes - a duplicated genome under selection. *Bmc Genomics, 17*(610).
683 doi:10.1186/s12864-016-2867-z

684 Korneliussen, T. S., Albrechtsen, A., & Nielsen, R. (2014). ANGSD: Analysis of next
685 generation sequencing data. *Bmc Bioinformatics, 15*(356). doi:10.1186/s12859-014-
686 0356-4

687 Kuhlwilm, M., Han, S., Sousa, V. C., Excoffier, L., & Marques-Bonet, T. (2019). Ancient
688 admixture from an extinct ape lineage into bonobos. *Nature Ecology & Evolution,*
689 *3*(6), 957-965. doi:10.1038/s41559-019-0881-7

690 Lamichhaney, S., Berglund, J., Almen, M. S., Maqbool, K., Grabherr, M., Martinez-Barrio,
691 A., . . . Andersson, L. (2015). Evolution of Darwin's finches and their beaks revealed
692 by genome sequencing. *Nature, 518*(7539), 371-375. doi:10.1038/nature14181

693 Lamichhaney, S., Han, F., Berglund, J., Wang, C., Almen, M. S., Webster, M. T., . . .
694 Andersson, L. (2016). A beak size locus in Darwin's finches facilitated character
695 displacement during a drought. *Science, 352*(6284), 470-474.
696 doi:10.1126/science.aad8786

697 Li, H., & Durbin, R. (2009). Fast and accurate short read alignment with Burrows-Wheeler
698 transform. *Bioinformatics, 25*(14), 1754-1760. doi:10.1093/bioinformatics/btp324

699 Malhi, Y., Franklin, J., Seddon, N., Solan, M., Turner, M. G., Field, C. B., & Knowlton, N.
700 (2020). Climate change and ecosystems: threats, opportunities and solutions.
701 *Philosophical Transactions of the Royal Society B - Biological Sciences,*
702 *375*(20190104). doi:10.1098/rstb.2019.0104

703 Marques, D. A., Meier, J. I., & Seehausen, O. (2019). A Combinatorial view on speciation
704 and adaptive radiation. *Trends in Ecology & Evolution, 34*(6), 531-544.
705 doi:10.1016/j.tree.2019.02.008

706 Meier, J. I., Marques, D. A., Mwaiko, S., Wagner, C. E., Excoffier, L., & Seehausen, O.
707 (2017). Ancient hybridization fuels rapid cichlid fish adaptive radiations. *Nature*
708 *Communications, 8*(11). doi:10.1038/ncomms14363

709 Meisner, J., & Albrechtsen, A. (2018). Inferring population structure and admixture
710 proportions in low-depth NGS data. *Genetics, 210*(2), 719-731.
711 doi:10.1534/genetics.118.301336

712 Meisner, J., Albrechtsen, A., & Hanghoj, K. (2021). Detecting selection in low-coverage
713 high-throughput sequencing data using principal component analysis. *Bmc*
714 *Bioinformatics, 22*(470). doi:10.1186/s12859-021-04375-2

715 Mevik, B. H., & Wehrens, R. (2007). The pls package: principal component and partial least
716 squares regression in R. *Journal of Statistical Software, 18*(2), 1-23.
717 doi:10.18637/jss.v018.i02

718 Moran, B. M., Payne, C., Langdon, Q., Powell, D. L., Brandvain, Y., & Schumer, M. (2021).
719 The genomic consequences of hybridization. *Elife, 10*. doi:10.7554/eLife.69016

720 Nenning, S. (1834). Die *Fische des Bodensees nach ihrer äussern Erscheinung*. Konstanz.
721 doi:10.3931/e-rara-72443

722 Nice, C. C., Gompert, Z., Fordyce, J. A., Forister, M. L., Lucas, L. K., & Buerkle, C. A.
723 (2013). Hybrid speciation and independent evolution of lineages of alpine butterflies.
724 *Evolution, 67*(4), 1055-1068. doi:10.1111/evo.12019

725 Nielsen, R., Korneliussen, T., Albrechtsen, A., Li, Y. R., & Wang, J. (2012). SNP calling,
726 genotype calling, and sample allele frequency estimation from new-generation
727 sequencing data. *Plos One, 7*(7). doi:10.1371/journal.pone.0037558

728 Nümann, W. (1972). The Bodensee: Effects of exploitation and eutrophication on the
729 Salmonid community. *Journal of the Fisheries Research Board of Canada, 29*(6),
730 833-884. doi:10.1139/f72-12

731 Nüsslin, O. (1907). *Coregonus wartmanni* Bloch und *macrophthalmus* Nüssl. -
732 Differentialdiagnose für das Stadium der Dottersackbrut. *Biologisches Zentralblatt,*
733 *27*, 440-447.

734 Pinsky, M. L., Eikeset, A. M., Helmerson, C., Bradbury, I. R., Bentzen, P., Morris, C., . . .
735 Star, B. (2021). Genomic stability through time despite decades of in cod on both
736 sides of the Atlantic. *Proceedings of the National Academy of Sciences of the United*
737 *States of America, 118*(15). doi:10.1073/pnas.2025453118

738 Prada, C., Hanna, B., Budd, A. F., Woodley, C. M., Schmutz, J., Grimwood, J., . . . Medina,
739 M. (2016). Empty niches after extinctions increase population sizes of modern corals.
740 *Current Biology, 26*(23), 3190-3194. doi:10.1016/j.cub.2016.09.039

741 Quinlan, A. R. (2014). BEDTools: The Swiss-army tool for genome feature analysis. *Current*
742 *Protocols in Bioinformatics, 47*(11.12.1-11.12.34). doi:
743 10.1002/0471250953.bi1112s47

744 R Core Team. (2018). R: A language and environment for statistical computing. Vienna,
745 Austria: R Foundation for Statistical Computing.

746 Racimo, F., Sankararaman, S., Nielsen, R., & Huerta-Sanchez, E. (2015). Evidence for
747 archaic adaptive introgression in humans. *Nature Reviews Genetics, 16*(6), 359-371.
748 doi:10.1038/nrg3936
749

750 Reilly, P. F., Tjahjadi, A., Miller, S. L., Akey, J. M., & Tucci, S. (2022). The contribution of
751 Neanderthal introgression to modern human traits. *Current Biology, 32*(18), PR970-
752 R983. doi:doi.org/10.1016/j.cub.2022.08.027

753 Rieseberg, L. H., Raymond, O., Rosenthal, D. M., Lai, Z., Livingstone, K., Nakazato, T., . . .
754 Lexer, C. (2003). Major ecological transitions in wild sunflowers facilitated by
755 hybridization. *Science, 301*(5637), 1211-1216. doi:10.1126/science.1086949

756 Rhymer, J. M., & Simberloff, D. (1996). Extinction by hybridization and introgression.
757 *Annual Review of Ecology and Systematics, 27*, 83-109.
758 doi:10.1146/annurev.ecolsys.27.1.83

759 Schweizer, W. (1894). Die Felchen des Bodensees und ihre natürliche und künstliche
760 Vermehrung. *Mitteilungen der Thurgauischen Naturforschenden Gesellschaft, 11*, 13-
761 26.

762 Schweizer, W. (1926). Der Gangfisch im Bodensee (Ober- und Untersee), sein Fang und
763 seine Pflege. *Mitteilungen der Thurgauischen Naturforschenden Gesellschaft, 26*, 3-
764 32.

765 Seehausen, O. (2004). Hybridization and adaptive radiation. *Trends in Ecology & Evolution,*
766 *19*(4), 198-207. doi:10.1016/j.tree.2004.01.003

767 Seehausen, O. (2006). Conservation: Losing biodiversity by reverse speciation. *Current*
768 *Biology, 16*(9). doi:10.1016/j.cub.2006.03.080

769 Seehausen, O., Takimoto, G., Roy, D., & Jokela, J. (2008). Speciation reversal and
770 biodiversity dynamics with hybridization in changing environments. *Molecular*
771 *Ecology, 17*(1), 30-44. doi:10.1111/j.1365-294X.2007.03529.x

772 Selz, O. M., Donz, C. J., Vonlanthen, P., & Seehausen, O. (2020). A taxonomic revision of
773 the whitefish of lakes Brienz and Thun, Switzerland, with descriptions of four new
774 species (Teleostei, Coregonidae). *Zookeys,* 989, 79-162.
775 doi:10.3897/zookeys.989.32822

776 Soraggi, S., Wiuf, C., & Albrechtsen, A. (2018). Powerful inference with the D-statistic on
777 low-coverage whole-genome data. *G3-Genes Genomes Genetics, 8*(2), 551-566.
778 doi:10.1534/g3.117.300192

779 Steinmann, P. (1950). Monographie der schweizerischen Koregonen. Beitrag zum Problem
780 der Entstehung neuer Arten. Spezieller Teil. *Schweiz. Z. Hydrologie, 12*(1), 340-491.
781 doi:doi:10.1007/BF02486030

782 Taylor, E. B., Boughman, J. W., Groenenboom, M., Sniatynski, M., Schluter, D., & Gow, J.
783 L. (2006). Speciation in reverse: morphological and genetic evidence of the collapse
784 of a three-spined stickleback (*Gasterosteus aculeatus*) species pair. *Molecular*
785 *Ecology, 15*(2), 343-355. doi:10.1111/j.1365-294X.2005.02794.x

786 Todesco, M., Pascual, M. A., Owens, G. L., Ostevik, K. L., Moyers, B. T., Hubner, S., . . .
787 Rieseberg, L. H. (2016). Hybridization and extinction. *Evolutionary Applications,*
788 *9*(7), 892-908. doi:10.1111/eva.12367

789 von Rapp, W. (1858). Ueber den Fang des Kilch (Coregonus acronius). *Jahreshefte des*
790 *Vereins für vaterländische Naturkunde in Württemberg, 14*, 328-331.

791 von Siebold, C. T. E. (1858). Kleinere Mittheilungen und Correspondenz - Nachrichten.
792 Ueber den Kilch des Bodensees (Coregonus acronius). *Zeitschrift für*
793 *wissenschaftliche Zoologie, 9*, 295-299.

794 Vonlanthen, P., Bittner, D., Hudson, A. G., Young, K. A., Muller, R., Lundsgaard-Hansen,
795 B., . . . Seehausen, O. (2012). Eutrophication causes speciation reversal in whitefish
796 adaptive radiations. *Nature, 482*(7385), 357-362. doi:10.1038/nature10824

797 Wahl, B., & Loffler, H. (2009). Influences on the natural reproduction of whitefish
798 (*Coregonus lavaretus*) in Lake Constance. *Canadian Journal of Fisheries and Aquatic*
799 *Sciences, 66*(4), 547-556. doi:10.1139/f09-019

800 Wellborn, G. A., & Langerhans, R. B. (2015). Ecological opportunity and the adaptive
801 diversification of lineages. *Ecology and Evolution, 5*(1), 176-195.
802 doi:10.1002/ece3.1347

803 Woods, P. J., Müller, R., & Seehausen, O. (2009). Intergenomic epistasis causes
804 asynchronous hatch times in whitefish hybrids, but only when parental ecotypes differ.
805 *Journal of Evolutionary Biology, 22*(11), 2305-2319. doi:10.1111/j.1420-
806 9101.2009.01846.x

Data accessibility

The raw sequencing files are accessible on ENA SRA (PRJEB53050). Additional supporting data (including the morphological data, genotype likelihood files and ENA sample accessions of all historical samples used) is deposited on the eawag research data institutional collection (doi:10.25678/0007FH). Scripts used for data analysis are available on GitHub (https://github.com/freidavid/Lake_Constance_Depth_Transect).

Author contributions

DF, OS and PGDF conceived of, designed, and conceptualized the study. PGDF managed and supervised the study. PR and DF together planned and run the field sampling and processed all specimen and samples for further analysis. DF analysed morphological and genomic data and visualized the results. DF wrote the original manuscript draft with input from OS and PGDF. All authors edited and reviewed the final manuscript.

Competing interest declaration

The authors declare no competing interests.

Supplementary Information

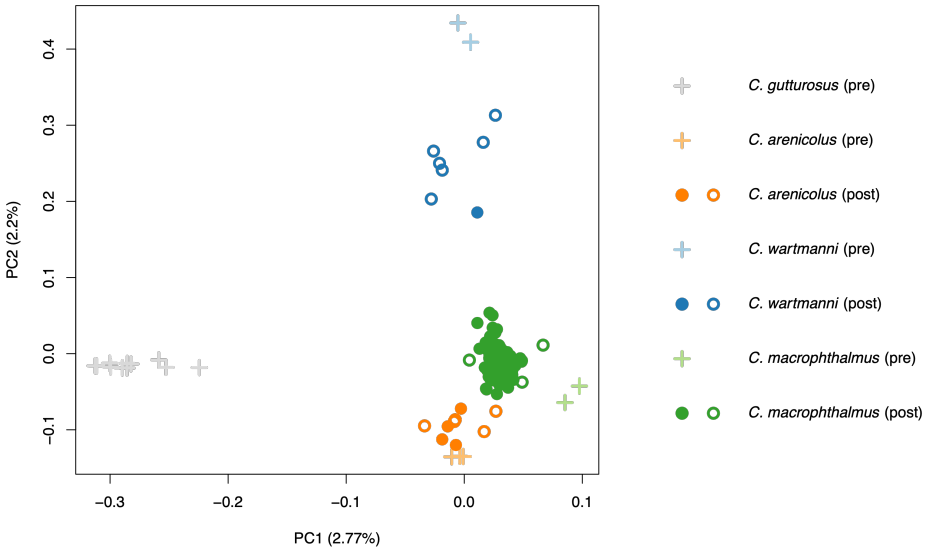

Supplementary Figure 1: PCA including all available Lake Constance samples. Grey is *C. gutturosus*, blue is *C. wartmanni*, green is *C. macrophthalmus* and orange is *C. arenicolus* (see legend to the right). Pre-eutrophication samples from Frei et al. (2022) are indicated with crosses, post-eutrophication samples are indicated with circles. Filled circles are samples caught in the depth transect sampling of this study, empty circles are from Frei et al. (2022).

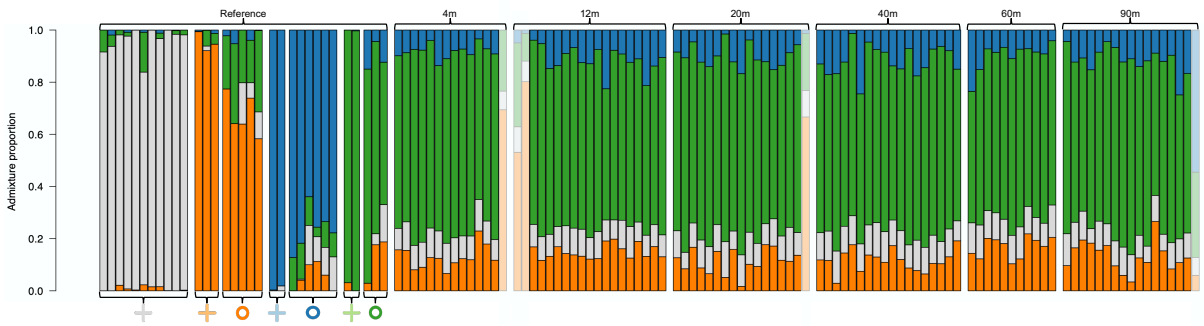

Supplementary Figure 2: Structure analysis, using all depth transect samples and all samples used in Frei et al. (2022). Grey is *C. gutturosus*, blue is *C. wartmanni*, green is *C. macrophthalmus* and orange is *C. arenicolus*. Reference samples from Frei et al. (2022) are divided into pre-eutrophication (crosses) and post-eutrophication (empty circles) samples. Samples are grouped into the six spawning depth populations, and individuals that were assigned to *C. wartmanni* or *C. arenicolus* are shaded.

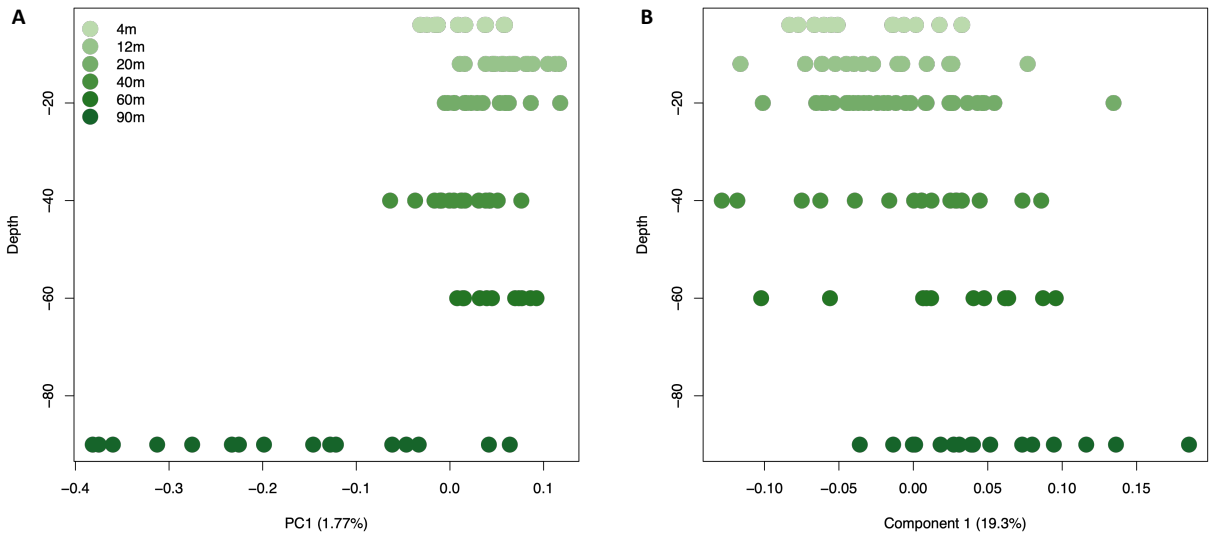

Supplementary Figure 3: A) Principal component 1 of the genomic PCA against depth including all caught *C. macrophthalmus* individuals. There was a significant correlation of PC1 with depth (rho=-0.37, p=0.0003). **B)** Component 1 of the partial least squares analysis against depth. There was a significant correlation of component 1 with depth (rho=-0.44, p=2e-6).

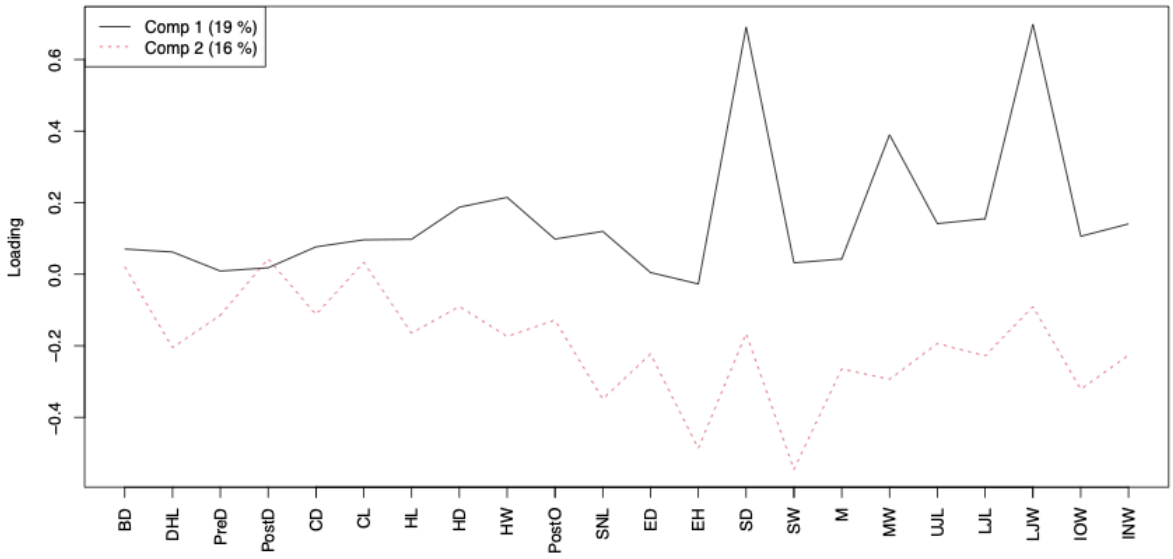

Supplementary Figure 4: Loadings of each trait of the partial least squares regression analysis (Figure 1D and Supplementary Figure 3B). All 22 morphometric traits and their loading on component 1 and 2 of the partial least squares regression analysis. The three traits with highest (positive) loadings on component 1 are LJW (lower jaw width), SD (snout depth) and MW (mouth width). The three traits with highest (negative) loadings on component 2 are SW (snout width), EH (eye height) and SNL (snout length).

Supplementary Table 1: D-statistic results for the test of introgression during eutrophication from *C. gutturosus* into each of the spawning depth populations. The table includes the ordering of the populations on the four-taxon topology used for the ABBA BABA test, as well as the resulting D values, Z-scores and p-values of the block-jackknife approach in 5 Mb blocks.

D	Z	P-value	P1	P2	P3	Outgroup
0.02	5.81	0.00	*C. macrophthalmus* pre (n=2)	4m	*C. gutturosus* pre (n=11)	*S. salar* (n=1)
0.01	4.78	0.00	*C. macrophthalmus* pre (n=2)	12m	*C. gutturosus* pre (n=11)	*S. salar* (n=1)
0.02	5.97	0.00	*C. macrophthalmus* pre (n=2)	20m	*C. gutturosus* pre (n=11)	*S. salar* (n=1)
0.02	6.31	0.00	*C. macrophthalmus* pre (n=2)	40m	*C. gutturosus* pre (n=11)	*S. salar* (n=1)
0.02	5.46	0.00	*C. macrophthalmus* pre (n=2)	60m	*C. gutturosus* pre (n=11)	*S. salar* (n=1)
0.01	4.19	0.00	*C. macrophthalmus* pre (n=2)	90m	*C. gutturosus* pre (n=11)	*S. salar* (n=1)

Supplementary Table 2: D-statistic results for the test of introgression during eutrophication from *C. wartmanni* into each of the spawning depth populations. The table includes the ordering of the populations on the four-taxon topology used for the ABBA BABA test, as well as the resulting D values, Z-scores and p-values of the block-jackknife approach in 5 Mb blocks.

D	Z	P-value	P1	P2	P3	Outgroup
0.01	2.82	0.00	*C. macrophthalmus* pre (n=2)	4m	*C. wartmanni* pre (n=2)	*S. salar* (n=1)
0.01	3.72	0.00	*C. macrophthalmus* pre (n=2)	12m	*C. wartmanni* pre (n=2)	*S. salar* (n=1)
0.01	4.05	0.00	*C. macrophthalmus* pre (n=2)	20m	*C. wartmanni* pre (n=2)	*S. salar* (n=1)
0.01	4.54	0.00	*C. macrophthalmus* pre (n=2)	40m	*C. wartmanni* pre (n=2)	*S. salar* (n=1)
0.01	3.72	0.00	*C. macrophthalmus* pre (n=2)	60m	*C. wartmanni* pre (n=2)	*S. salar* (n=1)
0.01	2.43	0.02	*C. macrophthalmus* pre (n=2)	90m	*C. wartmanni* pre (n=2)	*S. salar* (n=1)

Supplementary Table 3: D-statistic results for the test of introgression during eutrophication from *C. arenicolus* into each of the spawning depth populations. The table includes the ordering of the populations on the four-taxon topology used for the ABBA BABA test, as well as the resulting D values, Z-scores and p-values of the block-jackknife approach in 5 Mb blocks.

D	Z	P-value	P1	P2	P3	Outgroup
0.00	0.52	0.60	*C. macrophthalmus* pre (n=2)	4m	*C. arenicolus* pre (n=3)	*S. salar* (n=1)
0.00	-0.56	0.57	*C. macrophthalmus* pre (n=2)	12m	*C. arenicolus* pre (n=3)	*S. salar* (n=1)
0.00	-0.52	0.60	*C. macrophthalmus* pre (n=2)	20m	*C. arenicolus* pre (n=3)	*S. salar* (n=1)
0.00	-0.48	0.63	*C. macrophthalmus* pre (n=2)	40m	*C. arenicolus* pre (n=3)	*S. salar* (n=1)
0.00	-0.19	0.85	*C. macrophthalmus* pre (n=2)	60m	*C. arenicolus* pre (n=3)	*S. salar* (n=1)
0.00	-1.47	0.14	*C. macrophthalmus* pre (n=2)	90m	*C. arenicolus* pre (n=3)	*S. salar* (n=1)

Supplementary Table 4: Genes overlapping with any candidate SNP under selection between shallow and deep water (n=107), and their respective best Blast hits with an annotation of the genome of *Salmo salar*.

Gene name Alpine whitefish genome assembly (De-Kayne et al., 2020)	E value	Perc. identical	Accession	Description
snap_masked-PGA_scaffold11__203_contigs__length_63881516-processed-gene-283.13	2.00E-116	77.38	NP_001136192.1	RNA polymerase II subunit A C-terminal domain phosphatase SSU72
maker-PGA_scaffold11__203_contigs__length_63881516-snap-gene-418.12	0	89.89	XP_014023237.2	phosphatidylinositol 4-phosphate 3-kinase C2 domain-containing subunit beta-like
maker-PGA_scaffold11__203_contigs__length_63881516-snap-gene-480.10	0	85.07	XP_013987572.1	disks large-associated protein 4 isoform X1
maker-PGA_scaffold12__167_contigs__length_57740044-augustus-gene-463.9	3.00E-14	100	XP_045579496.1	gamma-aminobutyric acid receptor subunit beta-1 isoform X3
maker-PGA_scaffold14__173_contigs__length_55641933-snap-gene-414.19	0	97	XP_013997625.1	nucleoporin NUP188
maker-PGA_scaffold14__173_contigs__length_55641933-snap-gene-446.9	0	92.08	XP_013999495.2	lamin-B1
maker-PGA_scaffold15__168_contigs__length_54025139-augustus-gene-331.8	0	87.41	XP_045563145.1	kinesin-like protein KIF2A isoform X5
maker-PGA_scaffold15__168_contigs__length_54025139-snap-gene-398.18	0	85.17	XP_014026493.1	tenascin isoform X1
maker-PGA_scaffold17__183_contigs__length_51949489-snap-gene-114.25	0	87.47	XP_045562700.1	ARF GTPase-activating protein GIT2a isoform X2
maker-PGA_scaffold18__164_contigs__length_59907985-augustus-gene-424.0	0	87.9	XP_045544677.1	mucin-17
maker-PGA_scaffold19__147_contigs__length_54335267-snap-gene-386.8	0	91.1	XP_014004818.1	phosphatidylinositol 3-kinase regulatory subunit gamma-like isoform X1
maker-PGA_scaffold23__167_contigs__length_50329371-snap-gene-199.0	0	92.39	XP_014001415.2	laminin subunit beta-2 isoform X2
maker-PGA_scaffold23__167_contigs__length_50329371-snap-gene-487.17	1.00E-154	88.26	XP_045548802.1	FYVE, RhoGEF and PH domain-containing protein 1 isoform X1
maker-PGA_scaffold24__152_contigs__length_51033154-snap-gene-280.12	0	90.94	XP_014047632.1	rho-associated protein kinase 2 isoform X3
maker-PGA_scaffold24__152_contigs__length_51033154-snap-gene-396.16	0	85.99	XP_014051926.1	intersectin-2 isoform X1
maker-PGA_scaffold25__179_contigs__length_50922480-snap-gene-111.6	4.00E-156	87.74	XP_014025515.2	harmonin-like isoform X2
maker-PGA_scaffold26__192_contigs__length_48683376-snap-gene-73.17	0	87.65	XP_045545764.1	rap guanine nucleotide exchange factor 1 isoform X1
maker-PGA_scaffold26__192_contigs__length_48683376-snap-gene-229.16	0	91.17	XP_013984216.1	rab9 effector protein with kelch motifs
maker-PGA_scaffold26__192_contigs__length_48683376-snap-gene-381.32	0	72.26	XP_014051430.1	platelet-derived growth factor receptor beta
maker-PGA_scaffold28__172_contigs__length_48977775-snap-gene-133.10	2.00E-142	68.62	XP_014065728.2	consortin-like
maker-PGA_scaffold28__172_contigs__length_48977775-snap-gene-260.13	0	86.12	XP_014066184.1	protein jagged-2-like isoform X1
maker-PGA_scaffold29__157_contigs__length_48675208-snap-gene-407.12	0	84.5	XP_013991973.1	serine--tRNA ligase, cytoplasmic-like
maker-PGA_scaffold30__165_contigs__length_48446552-snap-gene-119.2	3.00E-73	72.61	XP_014034412.1	ras-related protein Rab-26
snap_masked-PGA_scaffold30__165_contigs__length_48446552-processed-gene-161.4	1.00E-36	92.31	XP_014034785.1	cGMP-dependent protein kinase 1 isoform X2
maker-PGA_scaffold30__165_contigs__length_48446552-snap-gene-177.15	2.00E-108	85.02	XP_014034899.2	mitochondrial import inner membrane translocase subunit Tim23

maker-PGA_scaffold33__143_contigs__length_40727438-augustus-gene-264.4	0.00E+00	94.94	XP_014014854.1	unnamed protein product
maker-PGA_scaffold38__206_contigs__length_33962415-snap-gene-84.0	3.00E-175	86.6	XP_014062081.1	EH domain-binding protein 1-like isoform X7
maker-PGA_scaffold38__206_contigs__length_33962415-snap-gene-286.7	0.00E+00	78.07	XP_014012100.1	phosphorylase b kinase regulatory subunit alpha, skeletal muscle isoform isoform X1
maker-PGA_scaffold4__243_contigs__length_45591172-snap-gene-365.20	0.00E+00	84.47	XP_045559993.1	1-phosphatidylinositol 4,5-bisphosphate phosphodiesterase eta-1 isoform X3
maker-PGA_scaffold7__351_contigs__length_68138733-snap-gene-159.14	0.00E+00	98.25	XP_013998328.2	homeobox protein Dlx5a-like

863